Heterogeneous sensitivity of human Acute Myeloid Leukemia to ß-catenin down-modulation

Arnaud Gandillet[#1], **Sophie Park**[#1], **François Lassailly**[1,†], **Emmanuel Griessinger**[1,†], **Jacques Vargaftig**[1], **Andrew Filby**[2], **T. Andrew Lister**[3], and **Dominique Bonnet**[1]

[1]Cancer Research UK Haematopoietic Stem Cell Group, London Research Institute, Cancer Research UK, London, UK

[2]Flow Cytometry Core Facility, London Research Institute, Cancer Research UK, London, UK

[3]Department of Medical Oncology, St. Bartholomew's hospital, Queen Mary University of London, London, UK

[#] These authors contributed equally to this work.

Abstract

Dysregulation of the Wnt/ß-catenin pathway has been observed in various malignancies, including acute myeloid leukemia (AML), where the over-expression of ß-catenin is an independent adverse prognostic factor. ß-catenin was found up-regulated in the vast majority of AML samples and more frequently localized in the nucleus of leukemic stem cells compared to normal bone marrow CD34^{+} cells. The knockdown of ß-catenin, using a short hairpin RNA (shRNA) lentiviral approach, accelerates ATRA-induced differentiation and impairs the proliferation of HL60 leukemic cell line. Using *in vivo* quantitative tracking of these cells, we observed a reduced engraftment potential after xenotransplantation when ß-catenin was silenced. However when studying primary AML cells, despite effective down-regulation of ß-catenin we did not observe any impairment of their *in vitro* long-term maintenance on MS-5 stroma nor of their engraftment potential *in vivo*. Altogether, these results demonstrate that despite a frequent ß-catenin up-regulation in AML, leukemia initiating cells might not be 'addicted' to this pathway and thus targeted therapy against ß-catenin might not be successful in all patients.

Keywords

leukemic stem cell; acute myeloid leukemia; xenotransplantation; Wnt/ß-catenin; leukemic culture initiating cells; whole body imaging

INTRODUCTION

Acute myeloid leukemia (AML) is a heterogeneous human disease defined by an accumulation of immature myeloblasts in the bone marrow and peripheral blood. Like other cancers, AML is a multi-step process characterized by the alteration of different pathways affecting cell proliferation and myeloid differentiation[1]. Over the last few years, it has been recognized that AML is maintained by leukemic stem cells (LSC) which are capable of initiating and sustaining leukemic growth[2-6]. These LSCs possess self-renewal capacity, as demonstrated by serial transplantation experiments. However, the detailed mechanisms and pathways responsible for the maintenance and/or acquisition of such properties remain poorly characterized. Different pathways have been postulated to be critical for LSC self-renewal such as Bmi1, Hox genes, Hedgehog, Notch and Wnt/ß-catenin[7-10]. The canonical Wnt/ß-catenin pathway[11] plays a critical role in self-renewal of HSCs and its dysregulation has been suggested in LSCs[12-13]. There is evidence that Wnt expression can inhibit the differentiation of HSCs, whereas over-expression of Axin (an antagonist of ß-catenin activation) has an inhibitory effect on Wnt signaling, which in turn results in a decrease of HSCs number[12]. Moreover, the addition of purified Wnt3a ligand in *ex vivo* culture has been used successfully to expand HSCs[14].

Nevertheless, the role of ß-catenin (encoded by the CTNNB1 gene) in normal murine HSCs remains controversial. Indeed, it has been reported that HSCs over-expressing ß-catenin acquired enhanced proliferation but were unable to engraft in irradiated mice[15]. A more recent study, focusing on the specific deletion of ß-catenin in different hematopoietic lineages, reported that although the loss of ß-catenin did not impair the formation of HSCs, these HSCs exhibited a deficit in long-term growth and maintenance. On the contrary, it has been reported that constitutive activation of ß-catenin causes a multilineage block in differentiation and compromises HSC maintenance by enforcing the cycling of HSCs, with the consequence of exhausting the long-term stem cell pool[16-17].

In a leukemia setting, Zhao *et al.* have elegantly shown that different ß-catenin levels lead to divergent effects in a Bcr-Abl model of leukemogenesis[18]. In their study, conditional ß-catenin deficient mice were generated and they showed that the loss of ß-catenin expression in the hematopoietic compartment decreased the incidence of chronic myeloid leukemia (CML). They were able to rescue this phenotype by ectopic ß-catenin expression, but interestingly only with low levels of ß-catenin. High doses of ß-catenin were detrimental to leukemogenesis. Therefore, the levels of ß-catenin, in addition to the activation status of the protein, can determine its complex pro- or anti-tumorigenic function. Most of the published work studying human LSC self-renewal and the implication of Wnt/ß-catenin pathway has examined CML[19]. In CML blast crisis, it has been shown that granulocyte-macrophage progenitors (GMP) express high levels of Bcr-Abl and had an activated Wnt-ß-catenin

pathway, with nuclear localization of ß-catenin[20]. As assessed via replating assays, they had enhanced replating capacity, which was inhibited by a specific Wnt pathway antagonist, Axin. CML-GMP also have self-renewal capacity in serially transplanted NOD/SCID mice and display an in-frame splice deletion of the GSK3ß kinase domain which could explain enhanced ß-catenin expression[21].

To date, no ß-catenin mutations have been found in AML, but there are other ways by which dysregulation of this pathway can occur. An increase in Flt3 signaling (via mutations/ amplifications) leads to Akt-mediated phosphorylation and inactivation of GSK3ß, resulting in the stabilization of ß-catenin and thus to increased activation of Wnt signaling[22]. An increase in Frizzled-4, a Wnt receptor that is induced by certain Flt3 mutations, leads to an activation of ß-catenin too, and consequently to an augmentation of TCF/LEF activity and MYC transcription[23]. Translocation products such as AML1-ETO and PLZF-RARα were also reported to activate the Wnt/ß-catenin pathway, by activating plakoglobin[24]. Furthermore, recent reports indicate that abnormal promoter methylation of specific Wnt inhibitors (*i.e.* sFRP1, sFRP2, SFRP4 sFRP5, WIF1, DKK3 and Hdpr1) can enhance Wnt/ß-catenin signaling in acute lymphoblastoid leukemia and AML[25-26].

The first piece of evidence for the importance of ß-catenin in AML patients comes from the work of Ysebaert *et al.*, who a few years ago retrospectively analyzed 118 patients for ß-catenin expression by Western Blot and correlated ß-catenin levels to survival. They identified ß-catenin as a new and independent negative prognostic factor predicting poor event-free survival and shortened overall survival[27]. At the level of the LSC in AML, only one report showed that the Wnt/ß-catenin signaling pathway was dysregulated, with a paradoxical over-expression of CK2, Axin, and APC, which are all negative regulators of this pathway[28].

Very recently however, in the study of Yeung *et al.* we concluded that in a mixed lineage leukemia (MLL) mouse model of AML, the level of ß-catenin was also critical for understanding the functional difference between pre-LSCs and LSCs. We went on to show that this pathway was also critical for the *ex vivo* maintenance of human leukemia[29].

Furthermore, Siapati *et al.* demonstrated the relevance of the Wnt/ß-catenin pathway in AML cell lines[30]. The question of whether or not this pathway is actually essential for the growth and maintenance of LSCs in all AML patients showing activation of ß-catenin still needs to be addressed. To this end, in the present study, we investigated the effect of down-modulation of ß-catenin in AML patients exhibiting different levels of ß-catenin activation, and show that not all patients are sensitive to this inhibition.

MATERIALS AND METHODS

Cells and human samples

The HL60 human leukemic cell line was obtained from American Type Culture Collection, USA. AML cells were obtained from patients at St Bartholomew's Hospital, London, UK after informed consent in accordance with the Declaration of Helsinki. Most samples were screened for their ability to engraft in immunodeficient mice before use in this study (Table

1). The protocol, as well as the obtention of cadaveric normal bone marrow cells, was approved by the East London Ethical Committee.

Human ß-catenin knock down

We used the pGIPZ lentivirus from OpenBiosystems (UK), which expresses a GFP cassette, as the empty vector. The target sequences from 5′ to 3′ was GCTCCTTCTCTGAGTGGTAAA (targeting the position 396-417 of human β-catenin gene, sh22 [29]). The same target sequence was inserted in another lentivector with an EF1α promoter instead of CMV (sh47). For the non-silencing scramble shRNA, CGGACTTGAATGGAATGATAAT was the target sequence.

Real time polymerase chain reaction (qPCR)

RNA samples were isolated using RNeasy Mini kit (Qiagen, UK) and reverse transcribed to cDNA using either Superscript III (Invitrogen, UK) or Omniscript Reverse transcriptase kits (Qiagen, UK). qPCRs were run in duplicate on an ABI 7900HT qPCR instrument equipped with SDS 2.3 software, using either SYBR Green or Power SYBR Green PCR master mix (Applied Biosystems, UK). Results were normalized to GAPDH or ß-actin via the $2^{-\triangle Ct}$ method.

Western blotting

Western blot analysis was performed using previously published standard techniques.

Hybond-C nitrocellulose membranes (Amersham Bioscience, GE Healthcare, UK) were probed with mouse anti-human ß-catenin clone14/Beta-catenin (BD Pharmingen, UK) or mouse anti-ß-actin (Sigma Aldrich, UK) antibodies. Donkey anti-mouse IgG-HRP sc-2314 (Santa Cruz Technology, USA) was used as a secondary antibody. Detection was achieved with Amersham ECL Plus Western Blotting reagent (GE Healthcare, UK) according to the manufacturer's instructions.

Flow cytometry analysis

Antibodies for flow cytometry were purchased from BD Biosciences (UK), except ß-catenin APC (R&D Systems, UK) and Alexa Fluor 647 anti-human CD38 clone HIT2 (Biolegend, UK), and used as described in their respective Materials & Method sections. The cells were analyzed using an LSRII cytometer (BD, UK) and DIVA software and/or FlowJo (Tree Star, Switzerland). Cells were sorted using either MoFlo (DakoCytomation, Fort Collins, CO, USA) or Aria (BD, UK) cell sorters. Gates were set up to exclude non-viable cells and debris. The negative fraction was determined using appropriate isotype controls.

For intracellular ß-catenin assessment, 5×10^6 cells were stained with PE-conjugated CD34 and Alexa Fluor 647-conjugated CD38 antibodies for 30 minutes at 4°C. Cells were then washed in phosphate buffer saline (PBS) containing 2% fetal calf serum (FCS) and fixed with paraformaldehyde 2% for 10 min before permeabilization for another 10 min in PBS with 0.1% Triton X-100 (Sigma Aldrich, UK). The cells were washed and stained with APC-conjugated anti-ß-catenin (1:25) for 1 hour. Then they were washed in PBS and resuspended in PBS with 0.2% FCS and 1 μg/ml 4′,6-diamidino-2-phenylindole (DAPI).

Imaging flow cytometric assessment of ß-catenin nuclear residency

The ImageStream imaging flow cytometer (Amnis, Seattle, WA, USA) was used to quantify the degree of ß-catenin nuclear internalization on large numbers of CD34⁻ and CD34⁺ subpopulations from AML and normal bone marrow (NBM) patients. Briefly, samples were first stained with fluorescently labelled antibodies against extracellular markers, followed by fixation, permeabilization then intracellular staining with ß-catenin FITC antibody for 1 hour. After washing, cells were resuspended in PBS with 0.2% FCS containing 0.1 μg/ml DAPI prior to acquisition on the ImageStream system (Amnis Corporation, USA). A minimum of 100000 total events were collected along with single color control files for spectral compensation. All compensation and data analysis were performed post-acquisition using the IDEAS 4.0 software package (Amnis). The fluorescence image-based method for quantifying nuclear residency of ß-catenin relies on the spectral isolation of ß-catenin signal image from the DAPI stained nuclear image[33]. Full details of how ß-catenin nuclear internalization was measured can be found in the supplemental information.

Lentivirus production and viral transduction

Viral particles were produced by transient calcium-phosphate co-transfection of 293T cells with the relevant vector plasmid, plus an encapsidation plasmid lacking Vif-, Vpr-, Vpu-, and Nef- accessory HIV-1 proteins (p 8.74), and a vesicular stomatitis virus envelope expression plasmid (pMDG2) (Plasmidfactory, Germany). Lentiviral particles were concentrated after ultracentrifugation at 19000 rpm (61600 *g*) for 150 min and stored at −80°C in StemSpan medium (StemCell Technologies, Canada).

Human HL60 cells were pre-stimulated overnight on MS5 stromal culture in StemSpan supplemented with recombinant human (rh) interleukin-3 (IL3), granulocyte colony stimulating factor (G-CSF), thrombopoietin (TPO) (Peprotech, London, UK; 20ng/mL each). Cells were then plated at 10^6 cells per ml in serum-free medium StemSpan (Stem Cell Technologies, Canada), supplemented with 4 μg/mL polybrene (Sigma Aldrich, UK) and the following rh cytokines: 100 ng/mL stem cell factor, 100 ng/mL Flt3 ligand, 60 ng/mL IL3, 10 ng/mL TPO. Multiplicity of infection (MOI) 10 to 30 for HL60 cell line was used for overnight transduction of cells either with control or silencing lentivirus in standard conditions of culture (humidified atmosphere, 37°C, 5% CO_2) and the next day cells were washed before any further analysis or plating.

Long-term culture (LTC) and limiting dilution assay (LDA)

For AML samples, after thawing, the pre-stimulation period was shortened to 4 hours without exposure to MS-5 cells, the other steps remaining unchanged (see Lentivirus production and viral transduction section). For LDA purposes, *ex vivo* culture of lentivirally transduced AML samples (MOI 30) was then performed on MS-5 stromal layer in the presence of 20 ng/ml each of rh IL3, G-CSF and TPO in MyeloCult H5100 media (StemCell Technologies, Canada) [34, 29].

Co-cultures were established in triplicates per condition and for each time point assessed (72 hours, and weeks 1, 2, and 3). Culture medium was replenished by a bi-weekly half-medium change. After trypsinization, cells were stained with various markers including anti-murine

Sca1-PE and anti-human CD45-APC antibodies (see flow cytometry analysis section) and only CD45^{+} Sca1^{−} cells were further analyzed and sorted.

For LDA assays, after the initial 3 weeks culture period, transduced AML cells were sorted for the presence of GFP and seeded in replicates onto a new MS-5 stromal layer at various seeding densities (ranging from 50 to 5000 cells per well of a 96-well plate). Scoring of positive wells for proliferation was done after 3 weeks.

Differentiation/morphology analysis

Differentiation of HL60 cells was induced with 1μM all-trans retinoic acid (ATRA) (Sigma Aldrich, UK) for 7 days[35]. After resuspension in PBS, cells were centrifuged in Cytofunnel devices at 500 rpm for 10 min and then stained with May-Grünwald Giemsa solution (Fluka, UK). Images from slides were acquired using a Zeiss Axiovert 40CFL microscope (364× magnification field) equipped with a Carl Zeiss Canon Power Shot A640 camera.

Cell cycle analysis, apoptosis, cell counts

For cell cycle analysis, cells were deprived of serum for 18 hours to synchronize them, then after centrifugation, were fixed in 2% paraformaldehyde for 10 min, permeabilized with 0.1% Triton X-100 for 10 min and resuspended in PBS containing 2% FCS and 1 μg/ml DAPI. Cell viability was assessed by DAPI and via Annexin V staining (BD Pharmingen, UK). CountBright absolute counting beads (Molecular Probes, Invitrogen, UK) were used to assess the absolute number of cells originally present in each tube.

Apoptotic cells were hypodiploid, G1 phase cells were identified as Ki67 positive and with 2n DNA content, cells in S phase were those with a DNA content ranging from 2n to 4n, and cells in G2/M phase had a 4n DNA content.

Colony forming unit (CFU) assays

Virally transduced HL60 were plated in triplicate at a density of 500 cells per ml of H4330 MethoCult media (StemCell Technologies, Canada) supplemented with 1% penicillin/streptomycin into individual 35mm diameter cell Petri dishes (Falcon, UK). The seeding density for AML samples (CFU blast assay) was 10000 cells per ml. In all cases, colonies were scored after 14 days in standard conditions of culture (humidified atmosphere, 37°C, 5% CO_2).

Animals and xenotransplantation (NOD/SCID assay)

All animal experiments were performed in accordance to the Home Office and Cancer Research UK regulations. NOD/SCID and NOD/SCID/β2-microglobulin null (NOD/SCID/β2m null) or NOD/SCID/gamma c null (NSG) male and female mice were obtained from Charles Rivers Laboratories (Moorgate, UK), hosted in micro-isolators and fed sterile food and acidified water. 8 to 12-week old mice were irradiated at 375cGy (^{137}Cs source) 16 to 24 hours before intravenous injection of cells. Mice were transplanted with 20000 to 400000 AML transduced cells.

Animals transplanted with primary AML cells were sacrificed at 12 weeks. Bone marrow from allfemurs, tibias, and pelvis were either flushed or crushed in PBS. Red blood cells were then lyzed with ammonium chloride.

Cells were stained with mouse anti-human antibodies against CD19, CD33, or CD45. Rat anti-mouse CD45 antibody was used as a negative marker. AML engraftment was considered as the $CD45^+CD33^+CD19^-$ population. Where there was a doubt as to the origin of engrafted cells, we assayed the cells for leukemia-specific mutations, where possible.

In vivo bioluminescence imaging

HL60 cells were first transduced with a lentiviral vector expressing the luciferase reporter gene (Firefly luciferase-RFP) (MOI 10). The TWR Luc–Fluc+RFP plasmid was a kind gift of Dr R. De Maria (Istituto Superiore di Sanità, Rome, Italy). In this construct, the luciferase cassette was placed under the control of CMV promoter and the RFP cassette was under the PGK promoter. RFP positive cells were then transduced with the lentivirus containing either the scramble control GFP or the ß-catenin GFP shRNA (MOI 10), and sorted again on GFP and RFP. An aliquot of these cells was analyzed on the IVIS Spectrum system to check for luciferase activity after addition of luciferin (150 μg/ml final concentration) (Caliper Life Science, USA). 8 to 10 weeks old NOD/SCID/β2m null mice were sublethally irradiated with 375 cGy 24 hours prior to intratibial injection of 5×10^6 luciferase-transduced HL60 cells. *In vivo* optical imaging was performed using IVIS Spectrum bioluminescence-fluorescence optical imaging system (Caliper Life Science, UK) at 24 hours, and after 1, 2, 3 and 4 weeks. Prior to imaging, each mouse was given an intraperitoneal injection of 125 mg/kg luciferin[32] (Caliper Life Science, UK). General anesthesia was induced with 3% isoflurane and the mouse was placed in a light-tight heated chamber. After acquiring bright-field images of each mouse, anterior and posterior luminescent images were then successively acquired with 1 to 5 min exposure time[36]. Optical images were displayed and analyzed with the IVIS Living Image software (Caliper Life Science, UK). Regions of interest were manually drawn around the bodies of the mice to assess the emitted signal intensity and sum of the anterior and posterior measurements were used as the total bioluminescence signal for each mouse. Optical signal was expressed as photon flux. In order to account for inter-individual variability, data were normalized by determining the proliferation index (as reflected by the ratio of BLI activity between 2 time points) for each animal.

Statistical analysis

Significances of human AML patient co-culture data, including LDA, and colony assays comparisons were determined as previously published[29]. Pearson's correlation coefficient was used to determine R^2 values whereas we tested for non-zero slope by calculating the appropriate t-statistic. The Kruskal-Wallis and Mann-Whitney *U* tests were used to assess the statistical significance of the differences observed between groups. The threshold for statistical significance (*) of *p* values was 0.05.

RESULTS

Expression and activation of ß-catenin in AML samples

We found by qPCR that ß-catenin was over-expressed compared to CD34^{+} normal bone marrow (NBM) in 13 out of 17 (76%) primary AML samples (Figure 1A). However, no correlation was found between ß-catenin expression and FAB subtype, karyotype, Flt3 or NPM status in our cohort. At the protein level, compared to NBM, the expression of intra-cellular ß-catenin in AML samples determined by flow cytometry was increased in 10 out of 17 (58%) samples (Figure 1B). In these samples and as expected due to ß-catenin post-translational regulation by the APC/GSK3ß/Axin complex, ß-catenin protein levels did not correlate with mRNA levels assessed by qPCR (Supplemental Figure S1). Indeed, out of the 13 samples in which ß-catenin was over-expressed at the mRNA level, only 8 (62%) also over-expressed ß-catenin at the protein level compared to NBM (data not shown). As ß-catenin was nonetheless found over-expressed at the mRNA and/or the protein level in 15 out of 17 samples (88%), we checked its expression in CD34^{+} and CD34^{−} cell fractions from both AML and NBM samples. There was no direct correlation between the percentage of CD34^{+} cells and the protein level of ß-catenin in AML samples ($R^2 = 0.12$, data not shown). Moreover, the mean fluorescence intensities (MFI) values for ß-catenin were not statistically significantly higher in the CD34^{+} populations than in their CD34^{−} counterparts, both for AML samples and NBM and also in AML *versus* NBM (Figure 1C).

We further confirmed that the Wnt/ß-catenin was actually activated, by determining the degree of ß-catenin nuclear residency in AML samples over-expressing ß-catenin, using the ImageStream system (Figures 2 and S2). Using this approach, we observed that proportionnaly ß-catenin was significantly more localized in the nucleus of CD34^{+} cells from all AML patients tested compared with those from NBM (Figure 2c), clearly reflecting an increase activation of the Wnt pathway. Considering that not all LSC reside within the CD34^{+} population (see Table 1 footnote), where appropriate, we determined the level of ß-catenin residency within the LSC compartment of patients to check whether ß-catenin was indeed active in the actual LSC fraction of the tested patients, as defined by their properties to engraft in NOD/SCID mice. Once again, we were able to record that significantly more ß-catenin was localized in the nucleus of the LSCs compared to that of CD34^{+} NBM cells (Figure 2D). Collectively, these data support the conclusion that in most but not all AML samples, Wnt/ß-catenin is over-activated and that this is a feature shared by LSCs regardless of their CD34 status.

The activation of other members in the Wnt/ß-catenin pathway was further confirmed by screening the mRNA levels of 84 genes related to this pathway for 7 patients in which ß-catenin was over-expressed compared to CD34^{+} NBM (Supplemental Table 1). As expected from Figure 1A, ß-catenin was vastly up-regulated in these samples. Genes upstream or downstream of ß-catenin were found differentially expressed, with target genes such as TCF1 and TCF3 being generally up-regulated, whereas TCF-4, LEF-1 and in some patients Cyclin D1 (unlike Cyclins D2 and D3) were under-expressed compared to CD34^{+} NBM, suggesting a feedback mechanism. Wnt ligands, Frizzled receptors, LPR5/6, Jun, MYC,

DKK1, were up-regulated in most patients whereas GSK3ß expression was differently affected depending on the patients studied.

Effect of the transduction of shRNA ß-catenin on HL60 proliferation *in vitro*

In order to understand the role of over-expression of ß-catenin in AML samples, we first down-modulated its expression in leukemic cell lines. The HL60 cell line was chosen because it could engraft in immunodeficient animals and because in our hands the knockdown efficiency was greater than in Fujioka cells which also express ß-catenin (data not shown).

HL60 cells were transduced and sorted at day 4 based on GFP expression to have a homogeneous population (purity > 97%) expressing either a control shRNA or a shRNA against ß-catenin (sh22 or sh47) (see Materials and Methods). ß-catenin was significantly and consistently found to be decreased at the mRNA level (80% to 95% knockdown) (Figure 3A, left panel), as well as by both flow cytometry and Western Blot at the protein level (70-90% knockdown) (Figure 3A middle and right panels respectively).

HL60 transduced cells showed only mild but consistent defects in proliferation in the initial stages (Figure 3B, left panel) with no difference in cell cycle status revealed at day 8 by flow cytometry (Figure 3B, right panel). qPCR analysis at day 8 indicated that the silencing was still effective and that apoptotic and pro-apoptotic genes were differentially expressed (Figure S3). Consistently, the proportion of cells positive for Annexin V was slightly greater in the knocked-down cells *versus* control (Figure 3C), however these effects did not increase over time. Indeed, the proliferation kinetics and apoptosis from GFP^{+} cells sorted at D8 (*i.e.* at the end point of original kinetics) were similar to that of control (data not shown).

We next looked at the potency of ß-catenin silenced HL60 cells to form hematopoietic colonies. Silenced cells were less potent to do so (Figure 3D, lower panel), moreover the morphology of the colonies (Figure 3D, upper panel) was consistent with such a defect in proliferation. To investigate the extent of ß-catenin silencing effects on myeloid differentiation, the production of granulocytes precursors was measured after the induction of myeloid differentiation with 1 μM ATRA for 4 days after transduction. Down-regulation of ß-catenin lead to a higher myeloid differentiation in HL60 cell line incubated with 1 μM ATRA, the cells being more mature as shown by an increased proportion of metamyelocytes and bigger cytoplasmic azurophilic granulations. As shown in Figure 3E, in the presence of ATRA, there was an average of 70% metamyelocytes/granulocytes in sh ß-catenin condition compared to 23% in control condition. Without ATRA, a maximum of 2% differentiated cells was observed in both conditions. We confirmed these findings by flow cytometry with an increase in the expression of the granulocytic marker CD11b, which was expressed in 94% of sh22-transduced cells against only 61% in control after ATRA exposure (data not shown). Similar findings were obtained with 1.3% dimethylsulfoxide- another inducer of differentiation (data not shown). Altogether, these data suggest an early impact of the down-regulation of ß-catenin in HL60.

Effect of ß-catenin silencing on HL60 behavior *in vivo*

To follow on our *in vitro* data, we wanted to assess whether HL60 leukemic cell proliferation was dependent *in vivo* on ß-catenin and thus if its silencing had an effect on bone marrow engraftment in NOD/SCID/β2m null recipient mice. After intra-tibial injection of double-transduced HL60 cells with luciferase either shRNA against ß-catenin or control, the proliferation and trafficking of the cells was non-invasively and longitudinally monitored by bioluminescence imaging (BLI) at different time points ranging from 24 hours to 4 weeks. This allows us to follow the tumor development based on luciferase signal intensity (Figure 4A). The endpoint data show a highly significant difference in cell proliferation between both conditions (p=0.01). As expected, ß-catenin silencing alone was not sufficient for preventing leukemic cells to proliferate since a 52-fold increase in BLI signal was observed between day 1 and week 4 in the ß-catenin silenced group. However, at least a sub-population of cells was affected, since in the control group the BLI signal increase was 447-fold *i.e.* about 8 times more than with silencing (Figure 4B). Despite individual variations, the average bone marrow engraftment at 4 weeks was also significantly affected with 20.2% in the control *versus* 3.3% in the ß-catenin silenced group (Figure 4C, p=0.02), corroborating the BLI data.

Taken together, these *in vivo* data demonstrate that, at least in HL60 cells, ß-catenin is involved in integration and/or transduction of signal emanating from the micro-environment and remains sensitive to environmental cues, whereas they could grow in a stroma-independent way *in vitro*. Having found such a crucial role for ß-catenin *in vivo*, we wondered whether this could also be true for primary AML samples.

Effect of ß-catenin silencing in primary AML samples *in vitro* and *in vivo*

A major critical point for assessing the effects of ß-catenin silencing in primary AML cells was to select patient samples with pre-assessed high engraftment potential in NOD/SCID or NSG mice, and high frequency of leukemic initiating cells (LIC), and of course for the purpose of our study, an increased level of ß-catenin. With these parameters we chose patients #1, #5 and #9. These patients had variable levels of ß-catenin over-expression - high (patient #1), medium (patient #5) and relatively low (patient #9) - among the 17 AML samples tested (see Figure 1).

The level of kncokdown of β-catenin mRNA was consistently greater than 80% after one week (Figure S4). Silencing of ß-catenin was also confirmed at the protein level by flow cytometry and ranged from 50% to 68% (data not shown). In order to directly assess the function of ß-catenin in LIC from primary AML samples, *in vitro* long-term culture (LTC) on MS-5 stroma and *in vivo* experiments were carried out. In a preliminary experiment, we observed that β-catenin knockdown significantly reduced the number of CFU-blasts *in vitro* (Figure S5), indicating that, like in the HL60 cell line, some progenitors were dependent on β-catenin signaling.

In LTC, the level of GFP+ cells gradually decreased in patients #5 and #1, but was stable in patient #9 (Figure 5A). However, we did not see any significant differences between the knockdown and the control group in any of the three patients tested. We then sorted GFP+

cells after 3 weeks and assessed by limiting dilution assay (LDA) the frequency of leukemia culture-initiating cells (LC-IC). The LC-IC frequency in knockdown *versus* control was similar in all three patients (Table 2). We thus confirmed that the down-regulation of β-catenin and of some downstream effectors was still effective by performing qPCR on GFP^{+} sorted cells at 3 weeks (Table 3). These data show that at least in the AML patients tested here, LC-ICs despite being efficiently targeted by β-catenin knockdown, were insensitive to this down-regulation. To confirm this lack of effect, we assessed the ß-catenin silencing effect on the AML engraftment potential in the NOD/SCID/β2m null mice. The engraftment of the transduced AML cells was assessed at week 12. We found no significant decrease in the level of engraftment for the ß-catenin silenced condition in all cases studied (Figure 5b), with a non significant decrease - even for patient #1 (expressing the highest level of ß-catenin) - in the proportion of GFP^{+} silenced cells compared to control (Figure S6). In patients #5 and #9 we were able to perform LDA of LC-ICs from GFP^{+} cells harvested from the primary transplanted mice. We again show no change in the frequency of LC-ICs when comparing knockdown to control (Table 4), and this was also the case when comparing the GFP[+] *versus* GFP[−] fraction for each condition (data not shown).

Taken together, our data show that the down-regulation of β-catenin has no effect on LC-ICs or LICs in the patients tested here.

DISCUSSION

The emerging role of Wnt signaling in AML has been increasingly investigated in recent years and ß-catenin has been suggested as a pivotal player in this disease[13].

In spite of the fact that ß-catenin protein levels could well differ from mRNA levels - probably due to the post-translational regulation of ß-catenin by the APC/GSK3ß/Axin complex- we report here that ß-catenin is over-expressed at the RNA and/or protein levels in a large portion of AML patients (15 out of 17) as compared to NBM. This confirms data from Ysebaert *et al.*[20]. However, whereas this group reported that patients with M4 or M5 FAB subtypes preferentially expressed ß-catenin, in our cohort we were unable to demonstrate any link between ß-catenin expression and FAB subtype, karyotype, Flt3 ITD or NPM mutation status. This may be explained by the relatively low number of AML patients included here in addition to the heterogeneity of AML samples. Individual variations were observed when looking at the mRNA level for the expression of genes involved in the Wnt/ß-catenin pathway. When looking at the more primitive LSC compartment, we found that the activation of the Wnt/ß-catenin pathway was higher in LSCs than in CD34^{+} NBM, as the localization of ß-catenin was more preferentially in the nucleus of LSCs compared to that of CD34^{+} NBM.

To test the impact of the loss of function of ß-catenin in AML, we first transduced HL60 leukemic cells with efficient shRNAs against ß-catenin and observed a decrease in cell proliferation, concomitant with a slight initial increase in apoptosis. At the mRNA level, the target genes of ß-catenin, like Cyclin D1 and MYC, were affected, as were some apoptotic and pro-apoptotic genes. Cyclins D2 and D3 genes were down-modulated, which is consistent with the observed reduced proliferation of HL60 cells over 8 days in culture.

Another effect that we noted upon silencing of ß-catenin, is the strikingly enhanced myeloid differentiation of the HL60 cell line after ATRA induction, which is consistent with previous data showing that the constitutive activation of ß-catenin blocks multilineage differentiation[17], resulting in a severe loss of $Gr1^+CD11b^+$ cells in recipient mice. Moreover, we show in the CFU-blast assays a decrease in the number as well as in the size of silenced cells compared to control. After *in vivo* transplantation in immunodeficient mice, we found that the engraftment potential of ß-catenin silenced HL-60 cells was significantly decreased, which is consistent with a recent report by Siapati *et al.*[30] Taken together, these *in vitro* and *in vivo* data using HL60 leukemic cells demonstrate that ß-catenin has a pivotal role in the control of the balance between proliferation and differentiation.

When looking at the effect of ß-catenin knockdown in AML patients' samples, we show that the silencing decreased significantly the number of CFU-blasts as previously reported[29], which indicates that at least some of the leukemic blasts/progenitors are sensitive to the knockdown of ß-catenin. In the first 3 weeks of co-culture, the number and percentage of GFP^+ cells diminished over time but not differently or preferentially in the silenced group over control conditions. Patient sample #9 was barely affected at all. This was true for the 3 samples studied despite their differences in the level of ß-catenin. Of note, primary LDA of LC-ICs of GFP^+ cells after 3 weeks did not reveal any difference compared to control. This finding is contrary to what we reported for two MLL translocated samples[29] using the same standard of techniques, where the frequency of LC-IC was greatly diminished after knocking down ß-catenin. In the samples tested in the present study, we further show that the pool of LSCs was unaffected. At 12 weeks the level of leukemic engraftment in mice was comparable between the two groups (silenced and control). Moreover, there was no impairment of the LC-IC frequency estimated by secondary LDA obtained from AML GFP^+ cells present in the primary transplants, which is the alternative to secondary transplants to test the self-renewal potential of the cells. Thus, this demonstrates that the self-renewal capacity of LSCs was not affected by the down-modulation of ß-catenin. To rule out a potential lack of efficient down-regulation of ß-catenin, we purified GFP^+ cells after 3 weeks of culture and show that at the mRNA level, ß-catenin was still efficiently silenced and target genes affected. What was particularly striking was the fact that even when the entire pathway was silenced, as in patient sample #9, we did not see any impact on either LC-ICs or LICs. Judging from the qPCR data, it seems that in some patients a compensatory mechanism potentially involved. It is also probable that other pathways such as Notch or PI3K can interact with Wnt signalling[13] and that at least in some cases the high levels of ß-catenin may be more a consequence of the dysregulation of other pathways in LSCs.

Our data indicate that ß-catenin targeting is unlikely to provide a universal target to eradicate AML LSCs in all AML patients. Nevertheless, our other report showing a sensitivity of MLL-translocated AML patients[29] along with recent data from Siapati *et al.*[30] suggest that for some subsets, ß-catenin silencing could be an option. Defining the group of patients who may be sensitive to ß-catenin inhibition on its own or via a multi-targeted therapy approach[37] will be important in designing personalised treatment approaches.

Supplementary Material

Refer to Web version on PubMed Central for supplementary material.

ACKNOWLEDGEMENTS

REFERENCES

1. Gilliland DG, Jordan CT, Felix CA. The molecular basis of leukemia. Hematology Am Soc Hematol Educ Program. 2004:80–97. [PubMed: 15561678]

2. Lapidot T, Sirard C, Vormoor J, Murdoch B, Hoang T, Caceres-Cortes J, et al. A cell initiating human acute myeloid leukaemia after transplantation into SCID mice. Nature. 1994; 367:645–648. [PubMed: 7509044]

3. Bonnet D, Dick JE. Human acute myeloid leukemia is organized as a hierarchy that originates from a primitive hematopoietic cell. Nat Med. 1997; 3:730–737. [PubMed: 9212098]

4. Ailles LE, Gerhard B, Kawagoe H, Hogge DE. Growth characteristics of acute myelogenous leukemia progenitors that initiate malignant hematopoiesis in nonobese diabetic/severe combined immunodeficient mice. Blood. 1999; 94:1761–1772. [PubMed: 10477702]

5. Ailles LE, Humphries RK, Thomas TE, Hogge DE. Retroviral marking of acute myelogenous leukemia progenitors that initiate long-term culture and growth in immunodeficient mice. Exp Hematol. 1999; 27:1609–1620. [PubMed: 10560908]

6. Feuring-Buske M, Gerhard B, Cashman J, Humphries RK, Eaves CJ, Hogge DE. Improved engraftment of human acute myeloid leukemia progenitor cells in ß 2-microglobulin-deficient NOD/SCID mice and in NOD/SCID mice transgenic for human growth factors. Leukemia. 2003; 17:760–763. [PubMed: 12682634]

7. Rizo A, Dontje B, Vellenga E, de Haan G, Schuringa JJ. Long-term maintenance of human hematopoietic stem/progenitor cells by expression of BMI1. Blood. 2008; 111:2621–2630. [PubMed: 18156489]

8. Sengupta A, Banerjee D, Chandra S, Banerji SK, Ghosh R, Roy R, et al. Deregulation and cross talk among Sonic hedgehog, Wnt, Hox and Notch signaling in chronic myeloid leukemia progression. Leukemia. 2007; 21:949–955. [PubMed: 17361218]

9. Dash AB, Williams IR, Kutok JL, Tomasson MH, Anastasiadou E, Lindahl K, et al. A murine model of CML blast crisis induced by cooperation between BCR/ABL and NUP98/HOXA9. Proc Natl Acad Sci USA. 2002; 99:7622–7627. [PubMed: 12032333]

10. Bansal D, Scholl C, Frohling S, McDowell E, Lee BH, Dohner K, et al. Cdx4 dysregulates Hox gene expression and generates acute myeloid leukemia alone and in cooperation with Meis1a in a murine model. Proc Natl Acad Sci USA. 2006; 103:16924–16929. [PubMed: 17068127]

11. Nusse, R. The Wnt Homepage. http://www.stanford.edu/group/nusselab/cgi-bin/wnt/

12. Reya T, Duncan AW, Ailles L, Domen J, Scherer DC, Willert K, et al. A role for Wnt signaling in self-renewal of haematopoietic stem cells. Nature. 2003; 423:409–414. [PubMed: 12717450]

13. Mikesch JH, Steffen B, Berdel WE, Serve H, Muller-Tidow C. The emerging role of Wnt signaling in the pathogenesis of acute myeloid leukemia. Leukemia. 2007; 21:1638–1647. [PubMed: 17554387]

14. Willert K, Brown JD, Danenberg E, Duncan AW, Weissman IL, Reya T, et al. Wnt proteins are lipid-modified and can act as stem cell growth factors. Nature. 2003; 423:448–452. [PubMed: 12717451]

15. Baba Y, Yokota T, Spits H, Garrett KP, Hayashi S, Kincade PW. Constitutively active ß-catenin promotes expansion of multipotent hematopoietic progenitors in culture. J Immunol. 2006; 177:2294–2303. [PubMed: 16887990]

16. Kirstetter P, Anderson K, Porse BT, Jacobsen SE, Nerlov C. Activation of the canonical Wnt pathway leads to loss of hematopoietic stem cell repopulation and multilineage differentiation block. Nat Immunol. 2006; 7:1048–1056. [PubMed: 16951689]

17. Scheller M, Huelsken J, Rosenbauer F, Taketo MM, Birchmeier W, Tenen DG, et al. Hematopoietic stem cell and multilineage defects generated by constitutive ß-catenin activation. Nat Immunol. 2006; 7:1037–1047. [PubMed: 16951686]

18. Zhao C, Blum J, Chen A, Kwon HY, Jung SH, Cook JM, et al. Loss of ß-catenin impairs the renewal of normal and CML stem cells in vivo. Cancer Cell. 2007; 12:528–541. [PubMed: 18068630]

19. Sloma I, Jiang X, Eaves AC, Eaves CJ. Insights into the stem cells of chronic myeloid leukemia. Leukemia. 2010; 24:1823–1833. [PubMed: 20861912]

20. Jamieson CH, Ailles LE, Dylla SJ, Muijtjens M, Jones C, Zehnder JL, et al. Granulocyte-macrophage progenitors as candidate leukemic stem cells in blast-crisis CML. N Engl J Med. 2004; 351:657–667. [PubMed: 15306667]

21. Abrahamsson AE, Geron I, Gotlib J, Dao KH, Barroga CF, Newton IG, et al. Glycogen synthase kinase 3ß missplicing contributes to leukemia stem cell generation. Proc Natl Acad Sci USA. 2009; 106:3925–3929. [PubMed: 19237556]

22. Brandts CH, Sargin B, Rode M, Biermann C, Lindtner B, Schwable J, et al. Constitutive activation of Akt by Flt3 internal tandem duplications is necessary for increased survival, proliferation, and myeloid transformation. Cancer Res. 2005; 65:9643–9650. [PubMed: 16266983]

23. Tickenbrock L, Schwable J, Wiedehage M, Steffen B, Sargin B, Choudhary C, et al. Flt3 tandem duplication mutations cooperate with Wnt signaling in leukemic signal transduction. Blood. 2005; 105:3699–3706. [PubMed: 15650056]

24. Muller-Tidow C, Steffen B, Cauvet T, Tickenbrock L, Ji P, Diederichs S, et al. Translocation products in acute myeloid leukemia activate the Wnt signaling pathway in hematopoietic cells. Mol Cell Biol. 2004; 24:2890–2904. [PubMed: 15024077]

25. Roman-Gomez J, Cordeu L, Agirre X, Jimenez-Velasco A, San Jose-Eneriz E, Garate L, et al. Epigenetic regulation of Wnt-signaling pathway in acute lymphoblastic leukemia. Blood. 2007; 109:3462–3469. [PubMed: 17148581]

26. Valencia A, Roman-Gomez J, Cervera J, Such E, Barragan E, Bolufer P, et al. Wnt signaling pathway is epigenetically regulated by methylation of Wnt antagonists in acute myeloid leukemia. Leukemia. 2009; 23:1658–1666. [PubMed: 19387464]

27. Ysebaert L, Chicanne G, Demur C, De Toni F, Prade-Houdellier N, Ruidavets JB, et al. Expression of beta-catenin by acute myeloid leukemia cells predicts enhanced clonogenic capacities and poor prognosis. Leukemia. 2006; 20:1211–1216. [PubMed: 16688229]

28. Majeti R, Becker MW, Tian Q, Lee TL, Yan X, Liu R, et al. Dysregulated gene expression networks in human acute myelogenous leukemia stem cells. Proc Natl Acad Sci USA. 2009; 106:3396–3401. [PubMed: 19218430]

29. Yeung J, Esposito MT, Gandillet A, Zeisig BB, Griessinger E, Bonnet D, et al. ß-catenin mediates the establishment and drug resistance of MLL leukemic stem cells. Cancer Cell. 2010; 18:606–618. [PubMed: 21156284]

30. Siapati EK, Papadaki M, Kozaou Z, Rouka E, Michali E, Savvidou I, et al. Proliferation and bone marrow engraftment of AML blasts is dependent on β-catenin signalling. Br J Haematol. 2010 e-pub ahead of print 1 Dec 2010; doi:10.1111/j.1365-2141.2010.08471.x.

31. Taussig DC, Miraki-Moud F, Anjos-Afonso F, Pearce DJ, Allen K, Ridler C, et al. Anti-CD38 antibody-mediated clearance of human repopulating cells masks the heterogeneity of leukemia-initiating cells. Blood. 2008; 112:568–575. [PubMed: 18523148]

32. Taussig DC, Vargaftig J, Miraki-Moud F, Griessinger E, Sharrock K, Luke T, et al. Leukemia-initiating cells from some acute myeloid leukemia patients with mutated nucleophosmin reside in the CD34(−) fraction. Blood. 2010; 115:1976–1984. [PubMed: 20053758]

33. Ortyn WE, Hall BE, George TC, Frost K, Basiji DA, Perry DJ, et al. Sensitivity measurement and compensation in spectral imaging. Cytometry A. 2006; 69:852–862. [PubMed: 16969805]

34. Schuringa JJ, Schepers H. Ex vivo assays to study self-renewal and long-term expansion of genetically modified primary human acute myeloid leukemia stem cells. Methods Mol Biol. 2009; 538:287–300. [PubMed: 19277587]

35. Matkovic K, Brugnoli F, Bertagnolo V, Banfic H, Visnjic D. The role of the nuclear Akt activation and Akt inhibitors in all-trans-retinoic acid-differentiated HL-60 cells. Leukemia. 2006; 20:941–951. [PubMed: 16617325]

36. Wang X, Rosol M, Ge S, Peterson D, McNamara G, Pollack H, et al. Dynamic tracking of human hematopoietic stem cell engraftment using in vivo bioluminescence imaging. Blood. 2003; 102:3478–3482. [PubMed: 12946998]

37. Luo J, Solimini NL, Elledge SJ. Principles of cancer therapy: oncogene and non-oncogene addiction. Cell. 2009; 136:823–837. [PubMed: 19269363]

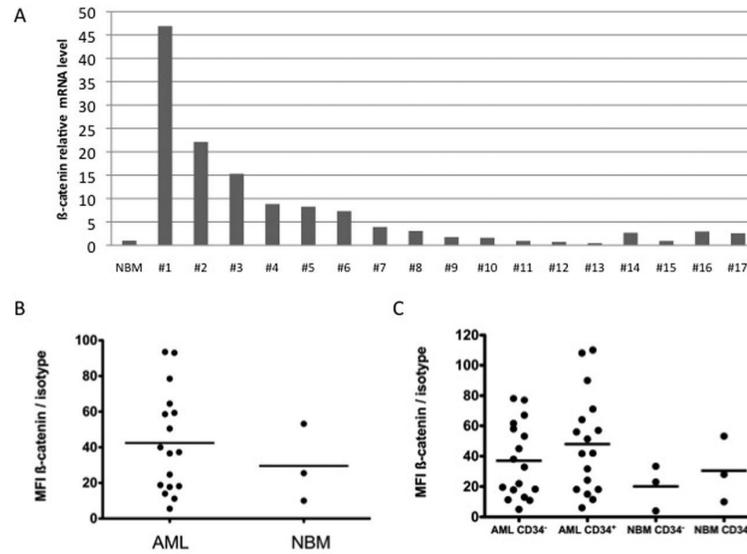**Figure 1. ß-catenin expression level in AML samples**
(A) Relative ß-catenin mRNA level in AML samples normalized to that of CD34$^+$ NBM.
(B) ß-catenin protein expression in 17 patients compared to NBM, as assessed by their ratio of fluorescence intensity (RFI, that is MFI ß-catenin / MFI isotype) (*p*=0.52). (C) ß-catenin expression in CD34$^+$ and CD34$^-$ cells of 17 AML patients *versus* NBM (*p*=0.44).
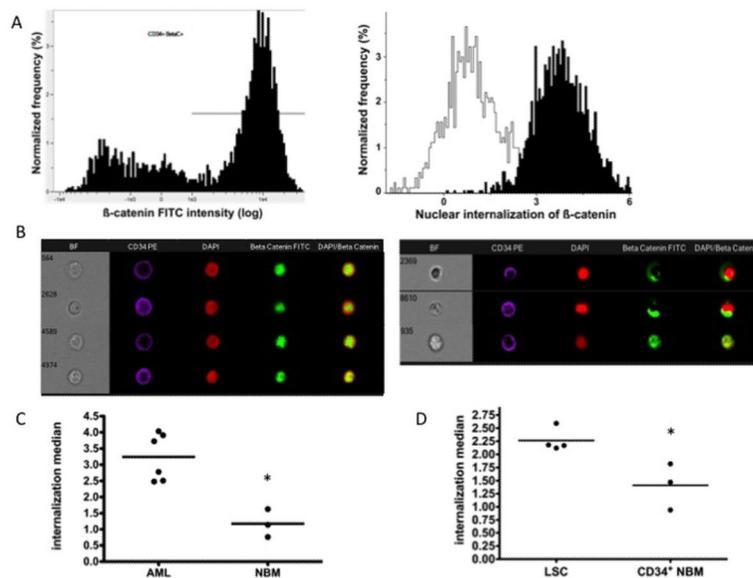
Figure 2. Measurement of nuclear internalised ß-catenin signal by ImageStream
(A) CD34^{+} gated events from AML sample (#15) were assessed for ß-catenin positivity and gated appropriately (left panel). CD34-PE^{+} ß-catenin^{+} events were then assessed for nuclear internalization of ß-catenin FITC signal within the DAPI-defined nuclear area of the cell (right panel; black: patient #15, white: NBM). The full process of measuring the nuclear internalization of ß-catenin is outlined in the supplemental materials and methods section. Increasing positive values reflect an increased proportion of the cells' ß-catenin signal residing within the DAPI[+] nuclear area. (B) Pseudo-colored spectrally decomposed compensated fluorescent and bright-field (BF) images representative of nuclear internalization scores for the same AML patient (#15) (internalization score 3.73, left) and NBM (internalization score 0.76, right) as in right panel A. (C) Median internalization scores for AML (n=6) *versus* NBM patients (n=3) (3.24 *versus* 1.18; *p*=0.02) and in (D) for LSC (n=4) *versus* NBM CD34^{+} (n=3) (*p*=0.02) (see also Table 1 footnote).
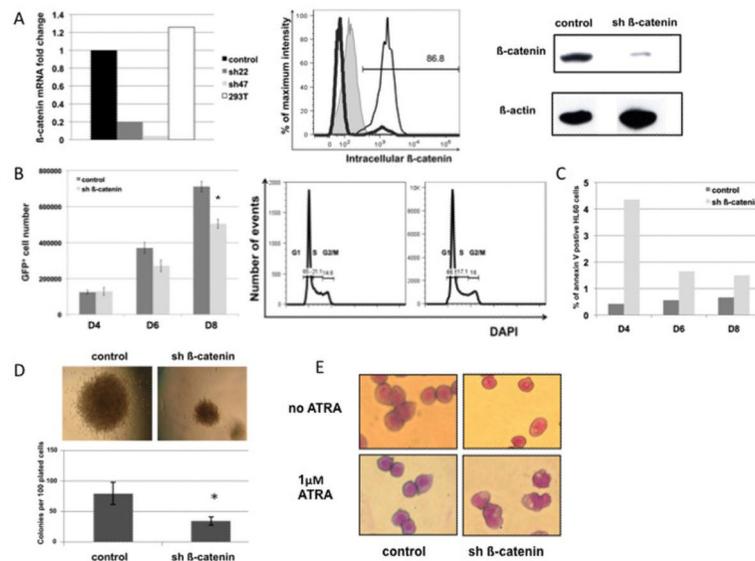
Figure 3. ß-catenin silencing in HL60 cell line

(A) Silencing of ß-catenin (left panel) at the mRNA level in HL60 sorted GFP+ cells at D4 post lentiviral transduction. 293T cells were used as an untransduced positive control; (mid panel) protein level obtained by flow cytometry in HL60 GFP+ cells. ß-catenin fluorescence intensity is shown for the isotype control (filled line), sh ß-catenin GFP+ (grey bold line) and control GFP+ (black line); (right panel) protein level obtained by Western Blot. Scramble construct was used as control, sh22 served as sh ß-catenin. (B) HL60 GFP+ proliferation kinetics at day 4, 6 and 8 (left panel). sh ß-catenin was sh47 *versus* respective scramble control. * $p<0.05$; (right panel) Cell cycle analysis at day 8. (C) Annexin V+ fraction in GFP+ HL60 cells as determined by flow cytometry on the same proliferation kinetics as in panel B. (D) Effect of ß-catenin knockdown on morphology, number of colonies ($p=0.01$) in CFU assay. Original magnification ×90 and (E) Myeloid differentiation assay. Cells were sorted for GFP+ for control or sh ß-catenin and exposed to 1μM ATRA for 4 days. Control: scramble construct; sh ß-catenin: sh22. Means are shown ± standard error of mean (SEM). * $p<0.05$.
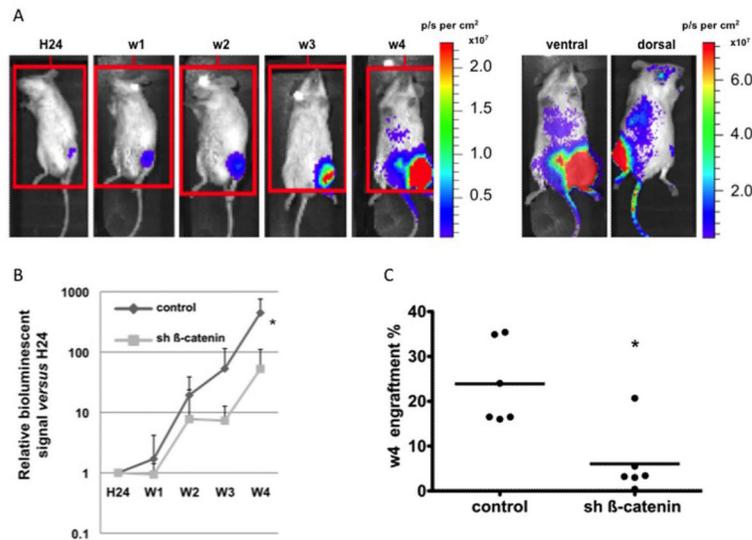
Figure 4. Longitudinal quantitative analysis of bioluminescence imaging (BLI)

NOD/SCID mice were injected intra tibia with HL60 cell line after double transduction either with scramble control and luciferase (Luc) reporter constructs or with sh ß-catenin and luciferase reporter constructs. (A) Representative ventral view of BLI kinetics in a mouse injected with control GFP+ Luc+ transduced HL60 cells (left panel). Ventral and dorsal views of the same mouse at week 4 are shown on the right panel. Optical signal was expressed as photon flux (photons per second (p/s)) per cm^2 body surface analyzed. (B) Relative BLI signal fold change *versus* day 0 (H24). The values are the mean of the sum of measured signal from both ventral and dorsal positions at each time point (weeks 1 to 4), divided by the initial basal value at 24 hours. Control: HL60 scramble GFP+ Luc+ mice (n=6). sh ß-catenin: HL60 sh22 GFP+ Luc+ mice (n=6). * *p*<0.05. (C) Effect of ß-catenin silencing on week 4 engraftment of HL60 in NOD/SCID mice (*p*=0.002). The engraftment was defined by the presence of CD45+CD33+CD19− population. * *p*<0.05.
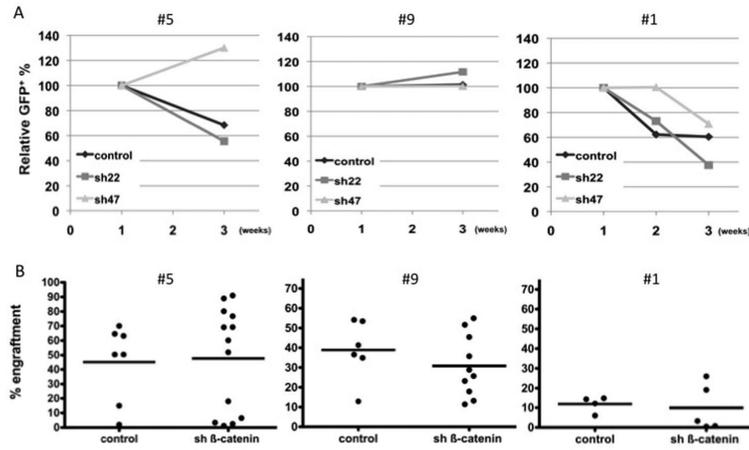
Figure 5. Effect of ß-catenin silencing in AML samples *ex vivo*
AML cells from patients #5, #9 and #1 were transduced with either control or the silencing ß-catenin lentivirus and co-cultured in triplicate on MS-5 stroma. (A) Relative GFP content in human CD45$^+$ cells up to 3 weeks of co-culture. Results are shown as normalised to 100% GFP at day 4. (B) AML LSC engraftment 12 weeks post-transplantation is not affected by ß-catenin silencing. Patient #5: control (n=7) *versus* sh ß-catenin (n=13) (*p*=0.57). Patient #9 control (n=6) *versus* sh ß-catenin (n=10) (*p*=0.36). Patient #1 control (n=4) *versus* sh ß-catenin (n=5) (*p*=0.73). Data were pooled from several independent experiments. Bone marrow engraftment was defined by the presence of CD45$^+$CD33$^+$CD19$^-$ population.

Table 1

Characteristics of AML patients' samples

	Age	Sex	FAB	WBC count	CD34 %	Karyotype
# 1	47.5	M	biphenotypic	314	3.5	Normal
# 2	50.2	F	M4	248	0.1	Normal, FLT3 ITD, NPM Mut
# 3	65.7	M	M1	2.2	84	+13
# 4	37	M	M0	62.2	69	−9q, +19
# 5	72.4	F	M2	116.8	0.14	Normal, NPM Mut
# 6	45.9	M	M4	165.2	86.9	11q23, Ins(6,11)
# 7	53.4	F	M2	9.6	2.74	Normal, NPM Mut, FLT3 ITD
# 8	64.3	F	M4Eo	67.5	60.3	Inv(16)
# 9	69.1	M	M1	98.7	0.3	Normal, NPM Mut
# 10	67.4	M	M1	126.7	3.3	+13, NPM Mut
# 11	59.5	F	M4Eo	61	65.6	Inv(16)
# 12	69.5	M	M5	56	9.4	N/A
# 13	64.3	F	M4	67.4	82.4	+12, +13
# 14	56.7	M	2nd AML	3.4	17.6	Complex
# 15	46.1	M	M4Eo	32.8	72.8	Inv(16), NPM Mut
# 16	65.5	M	M4Eo	6.3	50	Inv(16)
# 17	67.0	F	M2	112	2.01	Normal, NPM Mut

FAB indicates French-American-British classification. WBC: white blood cells count, expressed as $\times 10^9$ per litre of blood. NPM Mut: nucleosphosmin mutated. FLT3 ITD: FMS-like tyrosine kinase internal tandem duplication. Biphenotypic: lymphoid and myeloid markers. M4Eo: M4 with eosinophilia subtype. N/A: not assessed. Mutation analysis sequencing was performed using previously published methods. For each patient tested, we also investigated in parallel the phenotype of the LSCs. It has been shown in the late 1990s that AML is organized as a hierarchy that originates from a primitive LSC which has the CD34$^+$CD38$^-$ phenotype[2-5]. But lately we showed that the anti-CD38 antibody used for sorting can have a negative effect on the repopulating capacity of the LSC in *in vivo* models[31] and that CD34$^-$ AML cells can contain LSC, particularly in AML patients with mutated NPM[32]. Therefore, all four fractions of cells (CD34$^-$CD38$^-$, CD34$^+$CD38$^+$, CD34$^+$CD38$^-$ and CD34$^-$CD38$^+$) were tested for their ability to engraft in NSG mice. From these results, we determined the phenotype of the LSCs, which was used when looking at the expression and intra-cellular localization of ß-catenin.

Table 2

Limiting dilution assay for primary human AML cells after MS-5 long-term co-culture with or without β-catenin knockdown

Patient	Group	Frequency of target cells	95% confidence interval
#5	control	1 in 219	100-480
	sh22	1 in 278	129-598
	sh47	1 in 372	182-763
#9	control	1 in 1345	661-2737
	sh22	1 in 1490	726-3060
	sh47	1 in 1108	552-2227
#1	control	1 in 180	122-266
	sh22	N/A	N/A
	sh47	1 in 112	76-166

Results were observed at week 6 from GFP[+] populations sorted at week 3. Empty vector was used as control. N/A: Not assessed.

Table 3

Relative mRNA levels of beta catenin in GFP⁺ sorted patients' samples, after 3 weeks *ex vivo* co-culture on MS-5 stromal layer

Patient	#5			#9			#1		
	control	sh22	sh47	control	sh22	sh47	control	sh22	sh47
ß-catenin	1	0.07	0.93	1	0.21	0.37	1	0.02	0.01
Cyclin D1	1	1.1	0.9	1	0.22	0.45	1	40	3.8
Cyclin D2	1	10.1	1.4	1	0.1	0.23	1	<0.01	<0.01
Cyclin D3	1	0.75	2.6	1	0.2	2.6	1	<0.01	<0.01
BCL2	1	1.9	7.9	1	0.54	3.3	1	19.7	2
BAD	1	1.5	0.43	1	0.43	1.6	1	9.5	1.4
BAK	1	1.3	180.3	1	0.05	0.27	1	0.05	0.47
BCL XL	1	130.3	0.98	1	0.24	2.6	1	0.32	0.13
TCF3	1	0.82	1.2	1	0.04	0.29	1	80.7	9.2
SFRP4	1	0.6	1.3	1	0.11	0.32	1	49.5	5.3
DKK1	1	0.74	7.2	1	0.26	0.4	1	<0.01	<0.01
MYC	1	4.9	1.4	1	0.03	0.21	1	7.5	1.4
WNT5A	1	2.6	2	1	0.08	0.18	1	60.2	6.2

All data were normalised to β-actin and to respective control (empty vector) condition.

Table 4

LDA of LC-ICs after *ex vivo* culture of primary transplanted AML mice

Patient	Group	Frequency of target cells	95% confidence interval
#5	control	1 in 1332	547-3245
	sh22	1 in 912	409-2031
	sh47	1 in 1008	602-1688
#9	control	1 in 163	92-289
	sh22	1 in 175	99-306
	sh47	1 in 189	109-328

After lentiviral transduction, human AML cells were transplanted in NSG mice and sorted at week 12 for GFP[+]. LDA of LC-ICs was measured after an additional 3 weeks of culture from GFP[+] sorted populations plated on MS-5 stroma layer. Empty vector was used as control.